

Supplemental information

**Dysregulated innate immune signaling
cooperates with RUNX1 mutations to transform
an MDS-like disease to AML**

Laura Barreyro, Avery M. Sampson, Kathleen Hueneman, Kwangmin Choi, Susanne Christie, Vighnesh Ramesh, Michael Wyder, Dehua Wang, Mario Pujato, Kenneth D. Greis, Gang Huang, and Daniel T. Starczynowski

Supplemental Figure 1

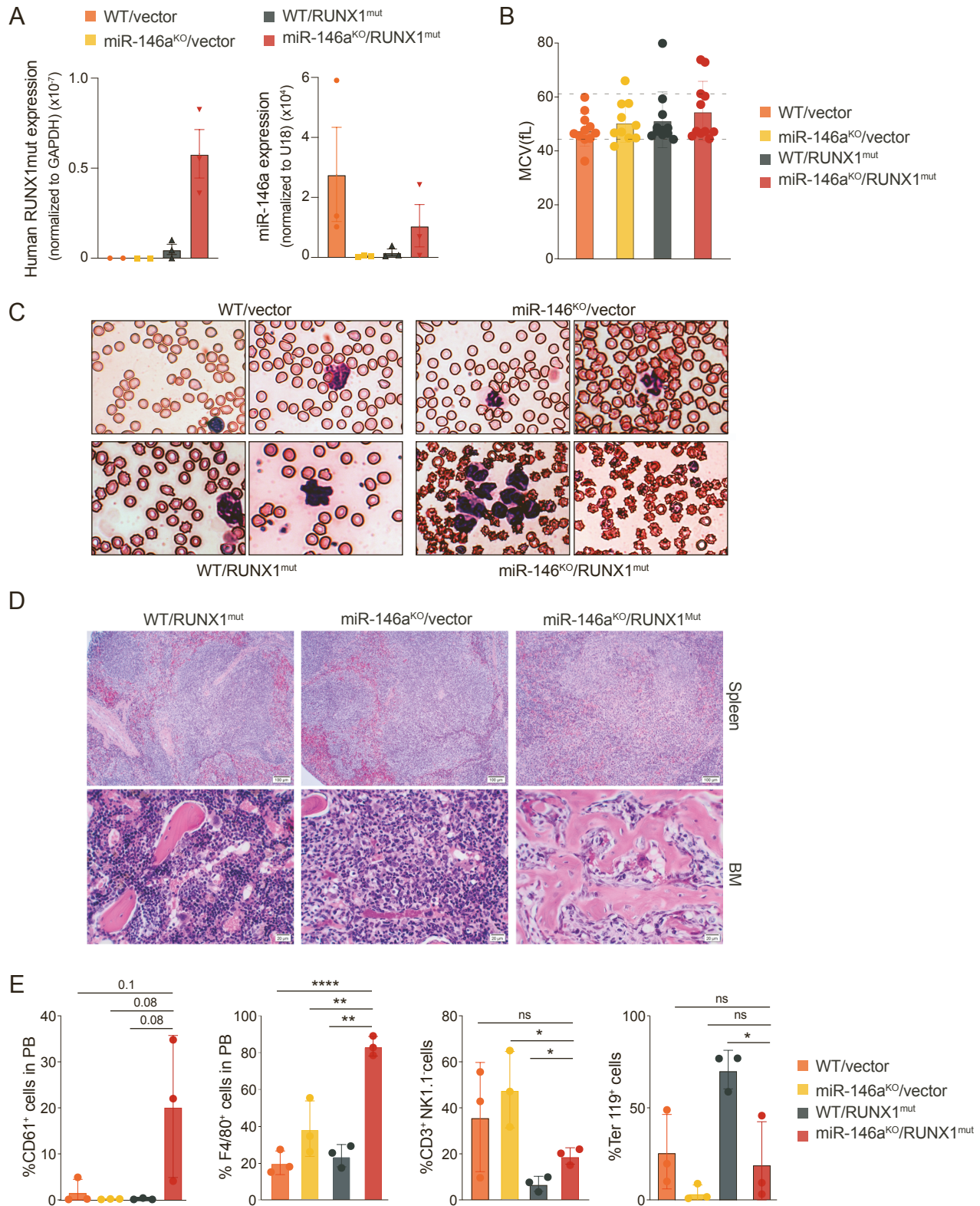
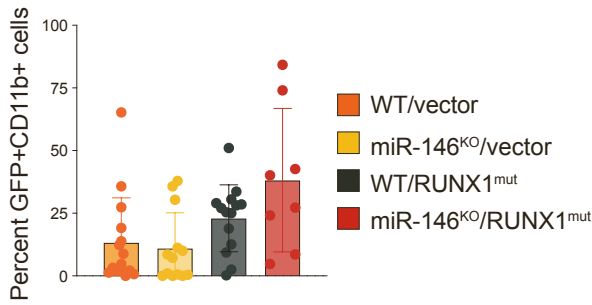


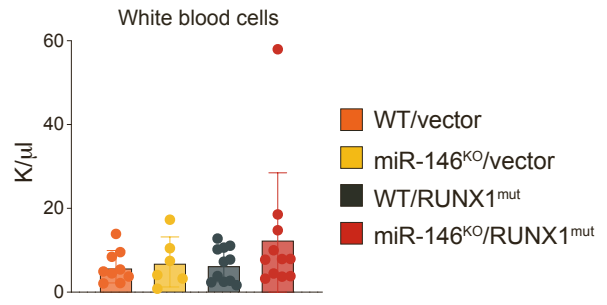
Figure S1, Related to Figure 1. Characterization of diseased mice. (A) Gene expression of human RUNX1^{mut} (left) and murine miR-146a (right) by quantitative PCR in BM aspirates of primary transplanted mice from the indicated mouse models (n = 3 per group). **(B)** Mean corpuscular volume values from primary transplanted mice. **(C)** Representative Giemsa staining from PB of mice 1 year post transplantation. **(D)** Representative H&E staining from spleen and BM from primary transplanted mice. Magnification 10X for spleen sections and 40X for BM. **(E)** Flow cytometric determination of cell surface expression profiles of CD61, Ter119, F4/80 and CD3/NK1.1 in circulation for primary BM transplanted mice. Error bars are the standard deviation. *, P<0.05; **, P<0.01; ***, P<0.001. Error bars represent the standard error of mean.

Supplemental Figure 2

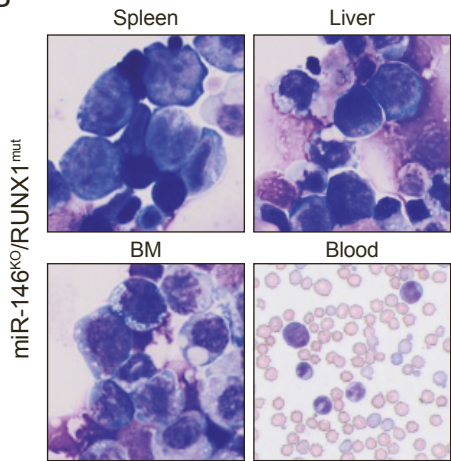
A



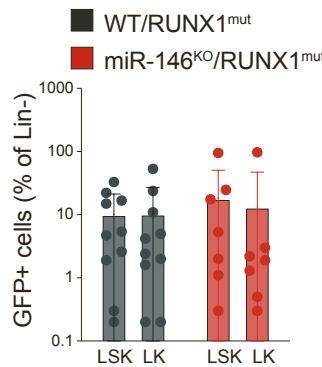
C



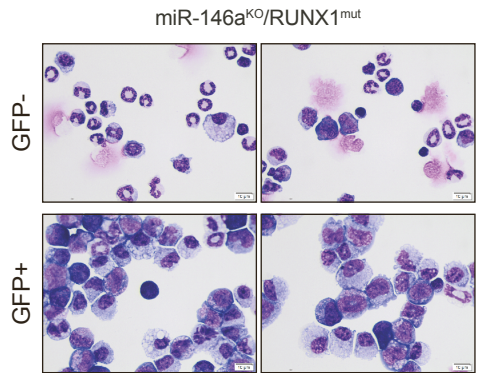
B



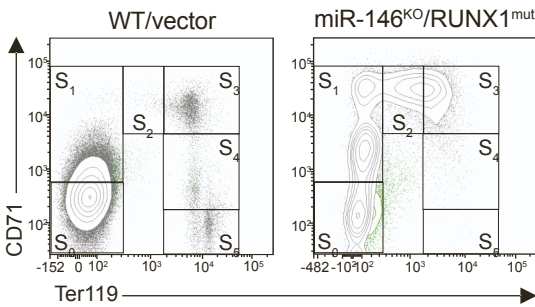
D



E



F



G

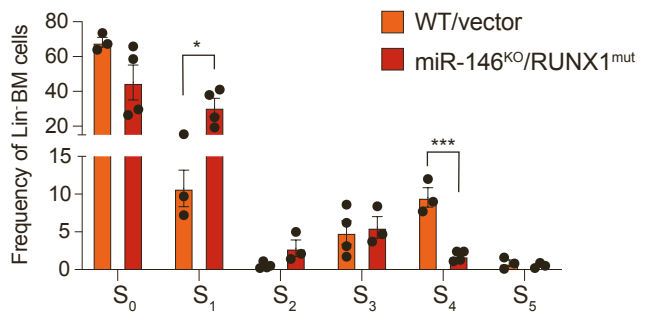


Figure S2, Related to Figure 2. miR-146a^{KO}/RUNX1^{mut} cells resemble AML. (A) Percentage of double CD11b⁻ and GFP-positive cells in PB post secondary transplantation measured by flow cytometry. **(B)** Representative Wright-Giemsa staining of spleen, BM, blood and liver cytopspins from secondary transplanted mice at time of death. Magnification 100X. **(C)** White blood cell counts from secondary transplanted mice at time of death. **(D)** Flow cytometric determination of the percentages of GFP positive LK and LSK cells expressed as percentage of lineage negative cells in secondary transplanted mice. **(E)** Representative images of Wright-Giemsa staining of BM cytopspins from sorted GFP positive and GFP negative cells of secondary transplanted miR-146a^{KO}/RUNX1^{mut} mice. **(F)** Representative flow cytometry plots showing CD71 and Ter-119 staining used to separate the stages of erythropoiesis for WT and miR-146a^{KO}/RUNX1^{mut} secondary transplanted mice. **(G)** Quantification of the erythroid subsets stages S₀–S₅ analyzed via flow cytometry from the bone marrow of secondary transplanted WT and miR-146a^{KO}/RUNX1^{mut} mice at time of death. A student's t-test was used to determine significance; *, P<0.01; ***, P<0.001. Error bars represent the standard error of mean.

Supplemental Figure 3

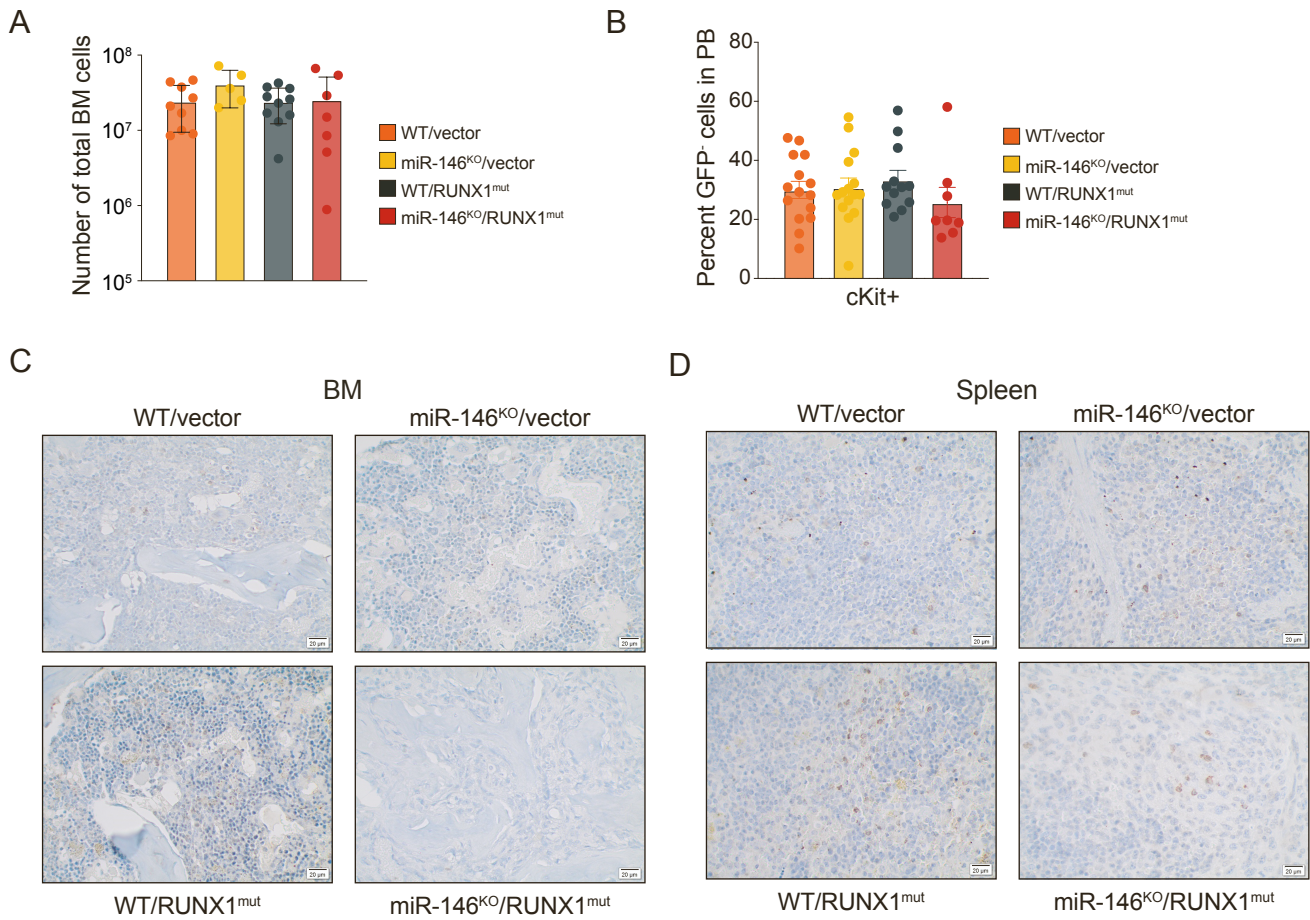


Figure S3, Related to Figure 3. Effects of miR-146a^{KO}/RUNX1^{mut} HSPCs on BM cellularity and colony formation. (A) Total number of BM cells evaluated in secondary transplanted mice (n = 5-10 mice per group). **(B)** GFP negative c-Kit⁺ cells in PB of secondary transplanted mice determined by flow cytometry. **(C-D)** Representative activated Caspase 3 immunohistochemistry staining of BM (C) and spleen (D) from primary transplanted mice. Magnification = 40X. Error bars are the standard deviation.

Supplemental Figure 4

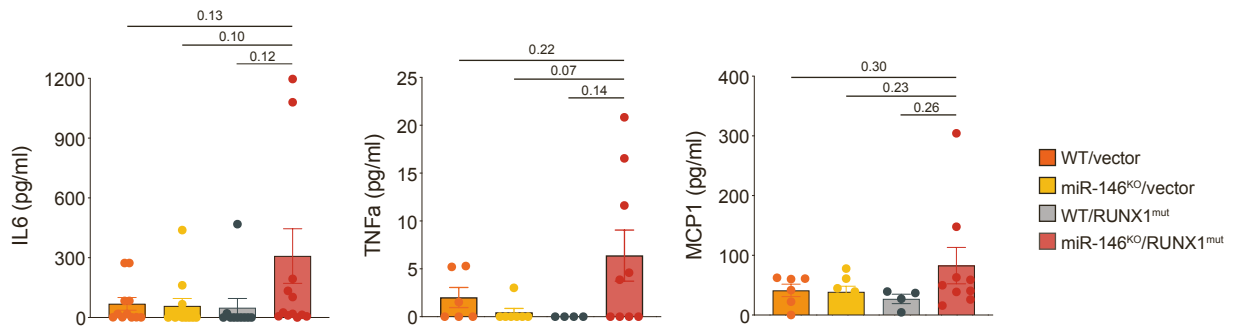


Figure S4, Related to Figure 3. Inflammatory cytokines are elevated in miR-146a^{KO}/RUNX1^{mut} mice. Plasma levels of the indicated cytokines (IL-6, TNF, and MCP1) in primary and secondary transplanted mice. Error bars represent the standard error of mean. Two-tailed unpaired t test.

Supplemental Figure 5

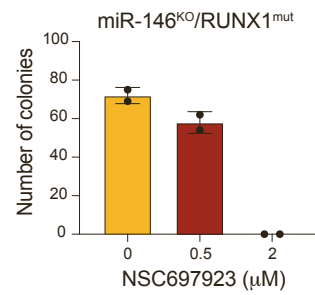


Figure S5, Related to Figure 5. Evaluation of the UBE2N inhibitor NSC697923 on miR-146a^{KO}/RUNX1^{mut} AML cells. Colony formation assay of miR-146a^{KO}/RUNX1^{mut} GFP+LSK AML cells treated with NSC697923 at the indicated doses. Error bars are the standard error of mean.